A Rigid-Plastic Hybrid PCM/FEM for Metal Forming Problems

YONG-MING GUO, SHUNPEI KAMITANI
Department of Mechanical Engineering
Kagoshima University
1-21-40 Korimoto, Kagoshima City, 890-0065
JAPAN
guoy@mech.kagoshima-u.ac.jp

Abstract: - Point collocation methods (PCM) have some advantages such as no mesh, no integration. While, the robustness of the point collocation methods is an issue especially when scattered and random points are used. To improve the robustness, some studies suggest that the positivity conditions can be important when using the PCMs. For boundary points, however, the positivity conditions cannot be satisfied, so that it is possible to get large numerical errors from the boundary points when using the point collocation methods. Specifically, the errors could arise in point collocation analyses with complicated boundary conditions. In this paper, by introducing a boundary layer of finite element in boundary domain of workpiece, unsatisfactory issue of the positivity conditions of boundary points can be avoided, and the complicated boundary conditions of metal forming can be easily imposed with the boundary layer of finite element. A modified MLS approximation is also proposed, its shape functions have Kronecker-delta property. Therefore, the unsatisfactory issue of the essential node condition can be avoided in the modified MLS approximation. To obtain very simple formulas of the shape function derivatives, the local coordinates are used in the hybrid PCM/FEM. An axisymmetric forging problem is analyzed by using the rigid-plastic hybrid PCM/FEM.

Key-Words: - Hybrid method, Meshless method, Point collocation method, FEM, Kronecker-delta property, Positivity conditions, Local coordinates, Metal forming.

1 Introduction

Metal forming problems are nonlinear and large deformation problems in general. They may be classified as bulk metal forming problems and sheet metal forming problems. The bulk metal forming problems used to be analyzed by the conventional rigid-plastic finite element methods (such as [1]). But the conventional rigid-plastic finite element methods have some shortcomings as follows: 1) Mesh generation is needed, which is costly. 2) Remeshing is needed when deformation is appreciable, while remeshing results in loss of accuracy.

Meshless methods are a group of numerical method for solving partial differential equations on regular or irregular distribution of points. Meshless methods require no costly mesh generation and remeshing. In addition, meshless methods allow arbitrary placement of nodes, therefore the solution and its derivatives may be obtained directly where they are needed. The early representatives of meshless methods are the diffuse element method [2], the element free Galerkin method [3], the reproducing kernel particle method [4], the hp-clouds method [5], the partition of unity method [6], the finite point method [7], the local boundary integral equation method [8], and the meshless local Petrov-Galerkin (MLPG) approach [9]. These meshless methods are mostly based on weak form (integral equations). In most meshless techniques, however, complicated non-polynomial interpolation functions are used which render the integration of the weak form rather difficult. Failure to perform the integration accurately results in loss of accuracy and possibly stability of solution scheme (specially, in nonlinear metal forming problems). The integration of complicated non-polynomial interpolation function costs much CPU time, too.

The point collocation method (PCM) is a kind of meshless method, which has no issues of the integration scheme, the integration accuracy and the integration CPU time. Therefore, the PCM has some advantages such as no mesh, no integration. Several PCMs based on different types of approximations or interpolations have been presented in the literature. Onate et al [7] have proposed a finite point method based on weighted least squares interpolations for the analyses of convective transport and fluid flow problems. Onate et al. [10] have also proposed a residual stabilization procedure, adequate for the finite

point method, and further extended the finite point method to the solution of the advective-convective transport equations as well as those governing the flow of compressible fluids. Aluru [11] has presented a PCM based on reproducing kernel approximations for numerical solution partial differential equations with appropriate boundary conditions. Jin et al. [12] have shown the robustness of collocation meshless methods can be improved by ensuring that the positivity conditions are satisfied when constructing approximation functions and their derivatives. Boroomand et al. [13] have presented a stabilized version of the finite point method to eliminate the ill-conditioning effect due to directional arrangement of the points. Patricio et al. [14] have given a numerical solution of a singularly perturbed two-point boundary-value problem using collocation. Atluri et al. [15] have presented a MLPG mixed collocation method by using the Dirac delta function as the test function in the MLPG method, and shown that the MPLG mixed collocation method is more efficient than the other MLPG implementations, including the MLPG finite volume method. Atluri et al. [16] have proposed a finite difference method, within the framework of the MLPG approach, for solving solid mechanics problems. Li et al. [17] have demonstrated the suitability and versatility of the MLPG mixed collocation method by solving the problem of topology-optimization of elastic structures. Chantasiriwan [18] has provided results of using the multiquadric collocation method to solve the lid-driven cavity flow problem. Wen et al. [19] have performed a geometrically nonlinear analysis of Reissner-Mindlin plate by using a meshless collocation method based on the smooth radial basis functions. Caraus et al. [20], [21] have studied the convergence and the stability of collocation methods for approximate solution of singular integro-differential equations. Kosec et al. [22] have explored the application of the mesh-free local radial basis function collocation method in solution of coupled heat transfer and fluid flow problems in Darcy porous media. Wu et al. [23] have developed a mesh-free collocation method based on differential reproducing kernel approximations for the three-dimensional analysis of simply-supported, doubly curved functionally graded magneto-electro-elastic shells under the mechanical load, electric displacement and magnetic flux. Yang et al. [24] have introduced a computational procedure based on meshless generalized finite difference method and serial magnetic resonance imaging data to quantify patient-specific carotid atherosclerotic plaque growth functions and simulate plaque progression. Spanulescu et al. [25] have analyzed the collocation method for solving the Hartree-Fock equations of the self-consistent field in large atomic and molecular systems, and have proposed a method for improving its performances by supplementary analytical and numerical quadrature. Khattak et al. [26] have presented an algorithm for the numerical solution of the generalized Hirota-Satsuma equations and Jaulent-Miodek equations based on meshless radial basis functions method using collocation points, called Kansa's method. Hon et al. [27] have applied the Hermite-based meshless collocation method based on radial basis functions to solve a default barrier model, which is a time-dependent boundary value problem with a singularity at the initial condition. Zahab et al. [28] have reported on the development and validation of a localized collocation meshless method to model laminar incompressible flows. To avoid the problem of excessive mesh distortions of the finite element method, Wieckowski [29] have used the material point method to solve problems of plastic forming, geomechanics and granular flow.

For boundary points, however, the positivity conditions cannot be satisfied, obviously, so that it is possible to get large numerical errors from the boundary points when using the PCMs. Specifically, the errors could arise in point collocation analyses with complicated boundary conditions. In this paper, a hybrid PCM/FEM is presented. By introducing a boundary layer of finite element in boundary domain of workpiece, unsatisfactory issue of the positivity conditions of boundary points can be avoided, and the complicated boundary conditions can be easily imposed with the boundary layer of finite element.

In the classical moving least-square (MLS) approximation, the shape functions have no Kronecker-delta property, so that the essential node condition cannot be imposed on boundaries. In this paper, a modified MLS approximation is proposed, its shape functions have Kronecker-delta property. Therefore, the unsatisfactory issue of the essential node condition can be avoided in the modified MLS approximation.

An axisymmetric forging problem is analyzed by using the rigid-plastic hybrid PCM/FEM.

2 Formulation

Let us assume a scalar problem governed by a partial differential equation:

$$D(u) = b, \quad in\,\Omega \tag{1}$$

with boundary conditions

$$T(u) = t, \quad on\,\Gamma_t \tag{2}$$

$$u - u_c = 0, \quad on\,\Gamma_u \tag{3}$$

to be satisfied in a domain Ω with boundary $\Gamma = \Gamma_t \bigcup \Gamma_u$, where D and T are appropriate differential operators, u is the problem unknown function (the velocity is adopted in this paper), b and t are external forces or sources acting over Ω and along Γ_t, respectively. u_c is the assigned value of u over Γ_u.

Let us assume Ω is divided into two subdomains, the interior domain Ω_{in} and the boundary domain Ω_{bo}. Surface between Ω_{in} and Ω_{bo} is defined as S (see Fig. 1).

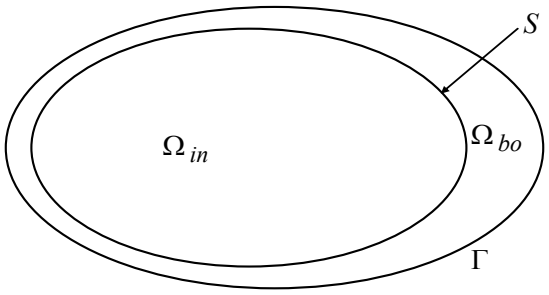

Fig. 1. Interior domain Ω_{in}, boundary domain Ω_{bo}, surface S and boundary Γ.

2.1 The Moving Least-Squares Approximation with Kronecker-Delta Property

Consider a small domain Ω_x, the neighborhood of a point x_1, which is located in Ω_{in}. Over Ω_x, u can be approximated by the MLS approximation. Over a number of randomly located nodes $\{x_i\}, i = 1, 2, \cdots, n$, the MLS approximation u^{h} of u can be defined by

$$u^{\mathrm{h}} = \mathbf{p}^{\mathrm{T}}(\mathbf{x})\boldsymbol{\alpha}, \qquad \forall \mathbf{x} \in \Omega_x \tag{4}$$

where $\mathbf{p}^{\mathrm{T}}(\mathbf{x}) = [p_1(\mathbf{x}) \;\; p_2(\mathbf{x}) \;\cdots\; p_m(\mathbf{x})]$ is a complete monomial basis of order m which is a function of the space coordinates $\mathbf{x} = [\mathbf{x} \;\; \mathbf{y} \;\; z]^{\mathbf{T}}$. $\boldsymbol{\alpha}$ is a vector of unknown polynomial coefficients,

$$\boldsymbol{\alpha} = [\alpha_1 \;\; \alpha_2 \;\cdots\; \alpha_m]^{\mathrm{T}}. \tag{5}$$

For example, for an axisymmetric problem,

$$\mathbf{p}^{\mathrm{T}}(\mathbf{x}) = \begin{bmatrix} 1 & r & z & r^2 & rz & z^2 \end{bmatrix} \tag{6}$$

this is a quadratic basis, and m=6.

A weighted least-square solution is obtained for $\boldsymbol{\alpha}$ from the following system of n equations in m unknown (n is larger than m):

$$\mathbf{u}^{\mathrm{h}} = \mathbf{H}\,\boldsymbol{\alpha} \tag{7}$$

$$\mathbf{u}^{\mathrm{h}} = \begin{bmatrix} u_1^{\mathrm{h}} & u_2^{\mathrm{h}} & \cdots & u_{\mathrm{n}}^{\mathrm{h}} \end{bmatrix}^{\mathrm{T}} \tag{8}$$

is a vector of the nodal MLS approximation of function u, and

$$\mathbf{H} = \begin{bmatrix} \mathbf{p}^{\mathrm{T}}(\mathbf{x}_1) & \mathbf{p}^{\mathrm{T}}(\mathbf{x}_2) & \cdots & \mathbf{p}^{\mathrm{T}}(\mathbf{x}_n) \end{bmatrix}^{\mathbf{T}}. \tag{9}$$

The classical least-square solution of the above over-constrained system does not guarantee exact satisfaction of any of the equations of equation (7). Non-satisfaction of the first equation would then mean $u_1^{\mathrm{h}} \neq \mathbf{p}^{\mathrm{T}}(\mathbf{x}_1)\boldsymbol{\alpha}$. Hence, a different approach to weighted least-squares solution can be adopted: Out of the n equations of equation (7), let the first equation (corresponding to node 1) be satisfied exactly and the rest in the least-square sense. This is done by using the first equation to eliminate α_1 from the rest of equations:

$$\alpha_1 = u_1^{\mathrm{h}} - (\alpha_2 r_1 + \alpha_3 z_1 + \alpha_4 {r_1}^2 + \alpha_5 r_1 z_1 + \alpha_6 {z_1}^2) \tag{10}$$

Substituting for α_1 in equation (7), the reduced system of equations can be obtained:

$$\overline{\mathbf{u}}^{\mathrm{h}} = \overline{\mathbf{H}}\,\overline{\boldsymbol{\alpha}} \tag{11}$$

$$\overline{\mathbf{u}}^{\mathrm{h}} = \begin{bmatrix} u_2^{\mathrm{h}} - u_1^{\mathrm{h}} & u_3^{\mathrm{h}} - u_1^{\mathrm{h}} & \cdots & u_{\mathrm{n}}^{\mathrm{h}} - u_1^{\mathrm{h}} \end{bmatrix}^{\mathrm{T}} \tag{12}$$

$$\overline{\mathbf{H}} = \begin{bmatrix} r_2 - r_1 & r_3 - r_1 & \cdots & r_n - r_1 \\ z_2 - z_1 & z_3 - z_1 & \cdots & z_n - z_1 \\ {r_2}^2 - {r_1}^2 & {r_3}^2 - {r_1}^2 & \cdots & {r_n}^2 - {r_1}^2 \\ r_2 z_2 - r_1 z_1 & r_3 z_3 - r_1 z_1 & \cdots & r_n z_n - r_1 z_1 \\ {z_2}^2 - {z_1}^2 & {z_3}^2 - {z_1}^2 & \cdots & {z_n}^2 - {z_1}^2 \end{bmatrix}^{\mathbf{T}}$$

$$= \begin{bmatrix} \overline{\mathbf{p}}^{\mathrm{T}}(\mathbf{x}_2) & \overline{\mathbf{p}}^{\mathrm{T}}(\mathbf{x}_3) & \cdots & \overline{\mathbf{p}}^{\mathrm{T}}(\mathbf{x}_n) \end{bmatrix}^{\mathrm{T}} \tag{13}$$

$$\overline{\boldsymbol{\alpha}} = [\alpha_2 \;\; \alpha_3 \;\cdots\; \alpha_m]^{\mathrm{T}}. \tag{14}$$

The coefficient vector $\overline{\boldsymbol{\alpha}}$ is determined by minimizing a weighted discrete L_2 norm, defined as:

$$J = \sum_{i=2}^{n} w(\mathbf{x}_i) \left[\overline{\mathbf{p}}^{\mathrm{T}}(\mathbf{x}_i)\,\overline{\boldsymbol{\alpha}} - \overline{u}_i \right]^2$$

$$= \left[\overline{\mathbf{H}}\,\overline{\boldsymbol{\alpha}} - \overline{\mathbf{u}} \right]^{\mathrm{T}} \mathbf{W} \left[\overline{\mathbf{H}}\,\overline{\boldsymbol{\alpha}} - \overline{\mathbf{u}} \right] \tag{15}$$

where $w(\mathbf{x})$ is the weight function, $\mathbf{x}_i$ denotes the value of $\mathbf{x}$ at node i, and matrices $\mathbf{W}$ is defined as

$$\mathbf{W}=\begin{bmatrix} w(\mathbf{x}_2) & 0 & \cdots & 0 \\ 0 & w(\mathbf{x}_3) & \cdots & 0 \\ \cdots & \cdots & \cdots & \cdots \\ 0 & 0 & \cdots & w(\mathbf{x}_n) \end{bmatrix}_{(n-1)\times(n-1)} \quad (16)$$

$$\bar{u}_i=\hat{u}_i-\hat{u}_1,\quad i=2,3,\cdots,n \quad (17)$$

$$\bar{\mathbf{u}}=\left[\hat{u}_2-\hat{u}_1\quad \hat{u}_3-\hat{u}_1\quad \cdots\quad \hat{u}_n-\hat{u}_1\right]^{\mathrm{T}} \quad (18)$$

where $\hat{u}_i, i=1,2,\cdots,n$ are the fictitious nodal values of the function u.

Minimizing J in equation (15) with respect to $\bar{\boldsymbol{\alpha}}$ yields

$$\bar{\boldsymbol{\alpha}}=\mathbf{A}^{-1}\mathbf{B}\bar{\mathbf{u}} \quad (19)$$

$$\mathbf{B}=\bar{\mathbf{H}}^{\mathrm{T}}\mathbf{W} \quad (20)$$

$$\mathbf{A}=\mathbf{B}\bar{\mathbf{H}}. \quad (21)$$

Substituting equation (19) into equation (11) gives a relation which may be written as

$$\bar{\mathbf{u}}^{\mathrm{h}}=\bar{\mathbf{H}}\mathbf{A}^{-1}\mathbf{B}\bar{\mathbf{u}}. \quad (22)$$

equation (10) can be rewritten as:

$$\alpha_1=u_1^{\mathrm{h}}-\mathbf{s}(\mathbf{x}_1)\bar{\boldsymbol{\alpha}} \quad (23)$$

$$\mathbf{s}(\mathbf{x}_1)=\begin{bmatrix} r_1 & z_1 & r_1^2 & r_1z_1 & z_1^2 \end{bmatrix}. \quad (24)$$

equation (4) can be written as:

$$u^{\mathrm{h}}=\alpha_1+\mathbf{s}(\mathbf{x})\bar{\boldsymbol{\alpha}} \quad (25)$$

$$\mathbf{s}(\mathbf{x})=\begin{bmatrix} r & z & r^2 & rz & z^2 \end{bmatrix}. \quad (26)$$

Substituting equation (19) and equation (23) into equation (25), the following equation can be obtained:

$$u^{\mathrm{h}}=u_1^{\mathrm{h}}+\mathbf{q}(\mathbf{x})\mathbf{A}^{-1}\mathbf{B}\bar{\mathbf{u}} \quad (27)$$

$$\mathbf{q}(\mathbf{x})=\mathbf{s}(\mathbf{x})-\mathbf{s}(\mathbf{x}_1) \quad (28)$$

$$\mathbf{q}(\mathbf{x}_1)=0 \quad (29)$$

$$u^{\mathrm{h}}(\mathbf{x}_1)=u_1^{\mathrm{h}}. \quad (30)$$

$\hat{\mathbf{u}}$ may be defined as:

$$\hat{\mathbf{u}}=\left[\hat{u}_1\quad \hat{u}_2\quad \cdots\quad \hat{u}_n\right]^{\mathrm{T}} \quad (31)$$

then, from equation (27), the following equation may be obtained:

$$u^{\mathrm{h}}=\mathbf{N}(\mathbf{x})\hat{\mathbf{u}} \quad (32)$$

$$\underset{1\times n}{\mathbf{N}(\mathbf{x})}=\left[1-\left(\underset{\mathbf{1}\times(\mathbf{m-1})}{\mathbf{q}(\mathbf{x})}\ \underset{(\mathbf{m-1})\times(m-1)}{\mathbf{A}^{-1}}\ \underset{(\mathbf{m-1})\times(n-1)}{\mathbf{B}}\ \underset{(\mathbf{n-1})\times 1}{\mathbf{1}}\right)\vdots\right.$$

$$\left.\underset{\mathbf{1}\times(\mathbf{m-1})}{\mathbf{q}(\mathbf{x})}\ \underset{(\mathbf{m-1})\times(m-1)}{\mathbf{A}^{-1}}\ \underset{(\mathbf{m-1})\times(n-1)}{\mathbf{B}}\right]. \quad (33)$$

In equation (33), **1** is vector of dimension (n-1) with all entries being equal to unity. Recall form equation (29), using this result in equation (33), the Kronecker-delta property of $\mathbf{N}(\mathbf{x})$ may be established:

$$\underset{1\times n}{\mathbf{N}(\mathbf{x}_1)}=\begin{bmatrix}1 & 0 & 0 & \cdots & 0\end{bmatrix} \quad (34)$$

which means that at node 1, the shape function for node 1 takes a value of unity and all other shape function take zero values. Therefore, equation (33) is the shape functions of the MLS approximation with Kronecker-delta property.

In this paper, the weight functions $w(\mathbf{x})$ may use a spline function as follows:

$$w(\mathbf{x})=1-6\left(\frac{d}{r_o}\right)^2+8\left(\frac{d}{r_o}\right)^3-3\left(\frac{d}{r_o}\right)^4,\quad 0\le d\le r_o \quad (35a)$$

$$w(\mathbf{x})=0,\qquad d\ge r_o \quad (35b)$$

where $d=|\mathbf{x}-\mathbf{x}_1|$ is the distance from point x to the center node x_1, and r_o is the radius of Ω_x, which is taken as a circle for a 2-D problem or an axisymmetric problem and its center is the point x_1.

2.2 The Local Coordinate System

As anisotropy of the point distribution in Ω_x, matrix **A** in equation (21) becomes ill-conditioned and the quality of the approximation deteriorates. In order to prevent such undesirable effect, a local coordinate system ξ,η [13] is chosen with origin at the point x_1 for an axisymmetric problem:

$$\xi=\frac{R-R_1}{\Delta_R},\qquad \eta=\frac{Z-Z_1}{\Delta_Z} \quad (36)$$

where Δ_R and Δ_Z denote maximum distances along R and Z measured from the point x_1 to exterior nodes in Ω_x. In equation (35a), spline function has now the following form in terms of the local coordinates:

$$w(\xi)=1-6\left(\frac{\sqrt{\xi^2+\eta^2}}{\rho}\right)^2+8\left(\frac{\sqrt{\xi^2+\eta^2}}{\rho}\right)^3-3\left(\frac{\sqrt{\xi^2+\eta^2}}{\rho}\right)^4 \quad (37)$$

$\rho=6$ is used in this paper and as usual $-1\le\xi\le 1, -1\le\eta\le 1$.

The matrix **A** is not longer dependent on the dimensions of Ω_x. The approximate function is also expressed in terms of the local coordinates as

$$u^h(\xi) = \mathbf{N}^{\mathrm{T}}(\xi)\hat{\mathbf{u}} = \sum_{i=1}^{n} N_i(\xi)\hat{u}_i \tag{38}$$

$\mathbf{A}^{-1}\mathbf{B}$ in equation (33) can be defined as $\mathbf{C}$:

$$\mathbf{C} = \mathbf{A}^{-1}\mathbf{B} \tag{39}$$

Then, from equation (33), entries of $\mathbf{N}(\mathbf{x})$ for the quadratic basis (m=6) can be written as:

$$\begin{aligned} \mathrm{N}_1(\mathbf{x}) = 1 - \Bigg[& (x - x_1)\sum_{i=1}^{n-1} C_{1i} + (y - y_1)\sum_{i=1}^{n-1} C_{2i} + \\ & \left(x^2 - {x_1}^2\right)\sum_{i=1}^{n-1} C_{3i} + (xy - x_1 y_1)\sum_{i=1}^{n-1} C_{4i} + \\ & \left(y^2 - {y_1}^2\right)\sum_{i=1}^{n-1} C_{5i} \Bigg] \end{aligned} \tag{40}$$

$$\begin{aligned} \mathbf{N}_{i+1}(\mathbf{x}) = {} & (x - x_1)C_{1i} + (y - y_1)C_{2i} + \left(x^2 - {x_1}^2\right)C_{3i} \\ & + (xy - x_1 y_1)C_{4i} + \left(y^2 - {y_1}^2\right)C_{5i} \\ & (i = 1, 2, \cdots, n-1) \end{aligned} \tag{41}$$

where C_{ji}, $(j = 1, 2, \cdots, 5;\ i = 1, 2, \cdots, n-1)$ are entries of $\mathbf{C}$. At the point x_1, because $\xi_1 = 0,\ \eta_1 = 0$, then the first-order derivatives of the shape function with the local coordinates can be obtained from equations (40) and (41):

$$\frac{\partial \mathbf{N}(\xi_1)}{\partial \xi} = \left[-\sum_{i=1}^{n-1} C_{1i} \quad C_{11} \quad C_{12} \quad \cdots \quad C_{1(n-1)} \right] \tag{42}$$

$$\frac{\partial \mathbf{N}(\xi_1)}{\partial \eta} = \left[-\sum_{i=1}^{n-1} C_{2i} \quad C_{21} \quad C_{22} \quad \cdots \quad C_{2(n-1)} \right] \tag{43}$$

From equations (42) and (43), we may see that formul as of the shape function derivatives with the local coor dinates are very simple, and in fact, it is a merit of the above-mentioned PCM using the local coordinates.

2.3 The Weighted Residual Method

Over Ω_{in} of Ω, the following weighted residual method is used:

$$\int_{\Omega_{in}} \hat{w}_i (D(\hat{\mathbf{u}}) - b) d\Omega = 0 \tag{44}$$

where $\hat{w}_i$ is a weight functions, and may be defined as follow in this paper.

$$\hat{w}_i = \delta_i \tag{45}$$

where δ_i is Dirac δ function.

Substituting equation (45) into equation (44), the following equation is obtained:

$$D(\hat{\mathbf{u}}) - b = 0 \tag{46}$$

Over the boundary domain Ω_{bo} of Ω, the FEM with one layer of finite element is used. The boundary conditions of equations (2) and (3) are imposed with the FEM, too.

By using the same nodes over the finite elements and in the small domain Ω_x, which center point x_1 is located on S or is close to S, the compatibility of nodal values of the nodes located on S and over Ω_{bo}, may be obtained.

2.4 The Positivity Conditions

The positivity conditions [12] on the approximation function $N_i(\mathbf{x})$ of equation (33) and its second-order derivatives are stated as

$$N_i(\mathbf{x}_j) \geq 0 \tag{47}$$

$$\nabla^2 N_i(\mathbf{x}_j) \geq 0, \quad j \neq i \tag{48}$$

$$\nabla^2 N_i(\mathbf{x}_i) \prec 0 \tag{49}$$

where $N_i(\mathbf{x}_j)$ is the approximation function of a point i evaluated at a point j.

Patankar [30] included the positivity conditions in a series of basic rules for the construction of finite differences and pointed out that the consequence of violating the positivity conditions give a physically unrealistic solution. It has been shown that the satisfaction of the positivity conditions ensures the convergence of the finite difference method with arbitrary irregular meshes for some class of elliptic problems [31]. It has been shown that the significance of the positivity conditions in meshless collocation approaches, and violation of the positivity conditions can significantly result in a large error in the numerical solution [12].

For a boundary point, a neighborhood centered on the point cannot be defined, so the positivity conditions on the boundary point cannot be satisfied, obviously. But for point x_1 on S, because it is not a boundary point, a small domain Ω_x, the neighborhood of the point x_1, can be defined. Therefore, the unsatisfactory issue of the positivity conditions of boundary points can be avoided in the hybrid PCM/FEM.

2.5 Formulation for Forming Problems

For an axisymmetric metal forming problem, the partial differential equations of mechanical equilibrium can be expressed as (in this paper, the body forces are omitted for simplicity):

$$\frac{\partial \sigma_R}{\partial R}+\frac{\partial \sigma_{RZ}}{\partial Z}+\frac{\sigma_R-\sigma_\theta}{R}=0 \quad (50a)$$

$$\frac{\partial \sigma_{RZ}}{\partial R}+\frac{\partial \sigma_Z}{\partial Z}+\frac{\sigma_{RZ}}{R}=0 \quad (50b)$$

where $\sigma_R, \sigma_Z, \sigma_\theta$ and σ_{RZ} are stress components. By the concept referring originally to a (nonlinear) viscous solid, the relating equation of stress vector σ and strain rate vector $\dot{\varepsilon}$ can be written as:

$$\sigma = \mathbf{D}\,\dot{\varepsilon} \quad (51)$$

for the rigid-plastic material

$$\mathbf{D}=\frac{\sigma_e}{\dot{\varepsilon}_e}\left[\frac{1}{3}\begin{bmatrix}2&0&0&0\\0&2&0&0\\0&0&2&0\\0&0&0&1\end{bmatrix}+\left(\frac{1}{g}-\frac{2}{9}\right)\begin{bmatrix}1&1&1&0\\1&1&1&0\\1&1&1&0\\0&0&0&0\end{bmatrix}\right] \quad (52)$$

where σ_e and $\dot{\varepsilon}_e$ denote the equivalent stress and the equivalent strain rate, respectively, and g is a material constant and a function of material density for slightly compressible materials.

Substituting the relationship equation of velocity and strain rate into equation (51), and then equations (50a) and (50b), the following non-linear equation of the mechanical equilibrium is derived:

$$\nabla^2\mathbf{u}+\mathbf{f}=\mathbf{0} \quad (53)$$

in which $\mathbf{u}$ is the velocity vector:

$$\mathbf{u}=[u \quad v]^{\mathrm{T}} \quad (54)$$

$$\mathbf{f}=[f_R \quad f_Z]^{\mathrm{T}} \quad (55)$$

where u and v denote velocity components, and

$$f_R=\left(\frac{3}{g}+\frac{1}{3}\right)\frac{\partial \dot{\varepsilon}_v}{\partial R}+\frac{1}{R}(\dot{\varepsilon}_R-\dot{\varepsilon}_\theta)+\left(\frac{1}{\sigma_e}\frac{\partial \sigma_e}{\partial R}-\frac{1}{\dot{\varepsilon}_e}\frac{\partial \dot{\varepsilon}_e}{\partial R}\right)\left[2\dot{\varepsilon}_R+\left(\frac{3}{g}-\frac{2}{3}\right)\dot{\varepsilon}_v\right]+\left(\frac{1}{\sigma_e}\frac{\partial \sigma_e}{\partial Z}-\frac{1}{\dot{\varepsilon}_e}\frac{\partial \dot{\varepsilon}_e}{\partial Z}\right)\dot{\gamma}_{RZ} \quad (56a)$$

$$f_Z=\left(\frac{3}{g}+\frac{1}{3}\right)\frac{\partial \dot{\varepsilon}_v}{\partial Z}+\frac{1}{R}\frac{\partial v}{\partial R}+\left(\frac{1}{\sigma_e}\frac{\partial \sigma_e}{\partial Z}-\frac{1}{\dot{\varepsilon}_e}\frac{\partial \dot{\varepsilon}_e}{\partial Z}\right)\left[2\dot{\varepsilon}_Z+\left(\frac{3}{g}-\frac{2}{3}\right)\dot{\varepsilon}_v\right]+\left(\frac{1}{\sigma_e}\frac{\partial \sigma_e}{\partial R}-\frac{1}{\dot{\varepsilon}_e}\frac{\partial \dot{\varepsilon}_e}{\partial R}\right)\dot{\gamma}_{RZ} \quad (56b)$$

where $\dot{\varepsilon}_v$ is the volumetric strain rate:

$$\dot{\varepsilon}_v=\dot{\varepsilon}_R+\dot{\varepsilon}_Z+\dot{\varepsilon}_\theta \quad (57)$$

Over Ω_{in}, by the MLS approximation, $\mathbf{u}$ in equation (48) can be written as:

$$u=\mathbf{N}^{\mathrm{T}}\,\hat{\mathbf{u}} \quad (58a)$$

$$v=\mathbf{N}^{\mathrm{T}}\,\hat{\mathbf{v}} \quad (58b)$$

Substituting equation (53) into equation (46), the partial differential equations on the nodal velocity components may be obtained:

$$\nabla^2\mathbf{N}^{\mathrm{T}}\hat{\mathbf{u}}+\mathbf{f}(\hat{\mathbf{u}},\hat{\mathbf{v}})=0 \quad (59a)$$

$$\nabla^2\mathbf{N}^{\mathrm{T}}\hat{\mathbf{v}}+\mathbf{f}(\hat{\mathbf{u}},\hat{\mathbf{v}})=0 \quad (59b)$$

In Ω_{bo}, the rigid-plastic FEM with one layer of finite element is used, and the boundary conditions of forming problems are imposed on Γ by using the rigid-plastic FEM, too.

3 Analyzed Results

In this section, an axisymmetric forging problem (see Fig. 2) is analyzed by using the rigid-plastic hybrid PCM/FEM. Vertical forging velocity of the upper die is 0.01m/s, and increment of time is taken as 0.2 s. The friction factor is taken as 0.05. The MLS approximation with the quadratic basis (m=6) is used. The nodal number n is taken as 9 in the PCM, and 4-noded quadratic finite element are adopted in the rigid-plastic FEM. The flow-stress-characteristics data of the material is given by the expression,

$$\sigma_{\mathrm{e}}=589.86\,\varepsilon_e^{\,0.0625} \quad MPa, \quad (\varepsilon_e \ge 0.002) \quad (60a)$$

$$\sigma_{\mathrm{e}}=400 \quad MPa, \quad (\varepsilon_e \le 0.002) \quad (60b)$$

where ε_e denotes the equivalent strain.

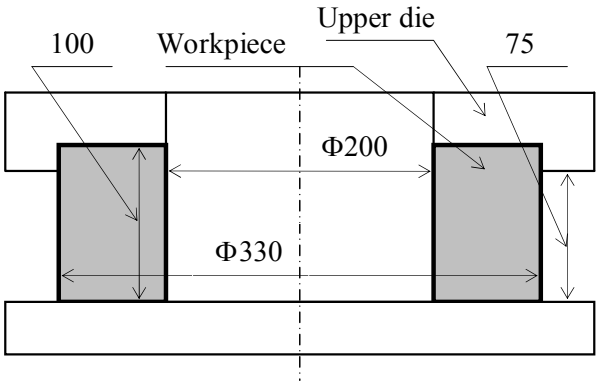

Fig. 2. Initial shape and dimensions of the workpiece and dies.

Figs. 3 and 4 show fields of the nodal velocity at 6% reduction and 10% reduction, respectively, and only one

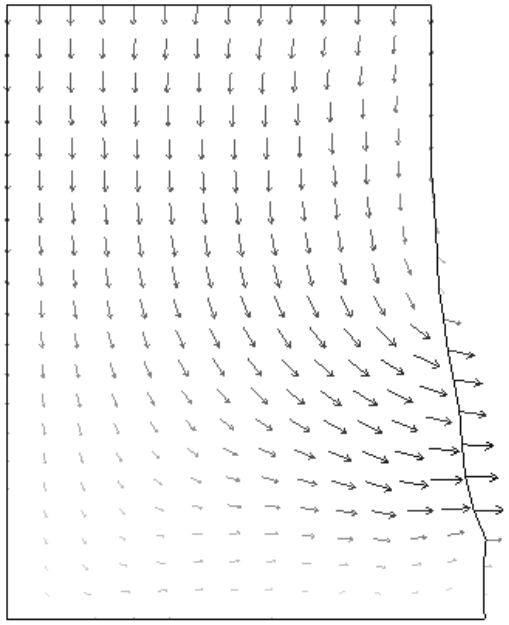

Fig. 3. Nodal velocity field at 6% reduction.

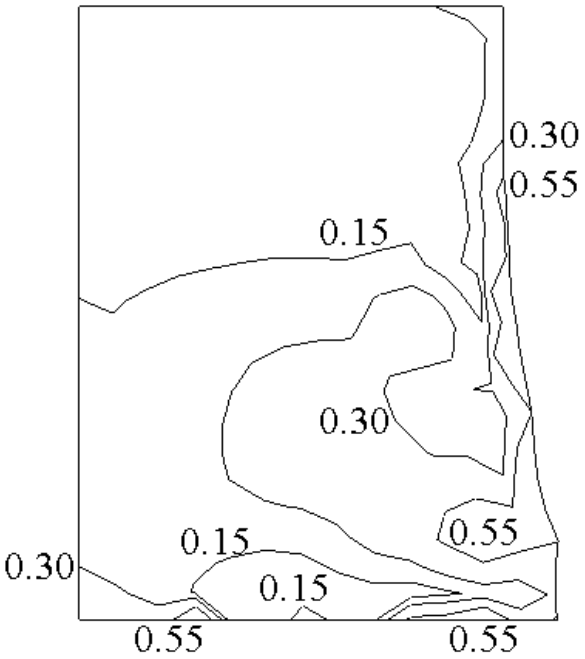

Fig. 5. Equivalent strain rate (1/s) at 6% reduction.

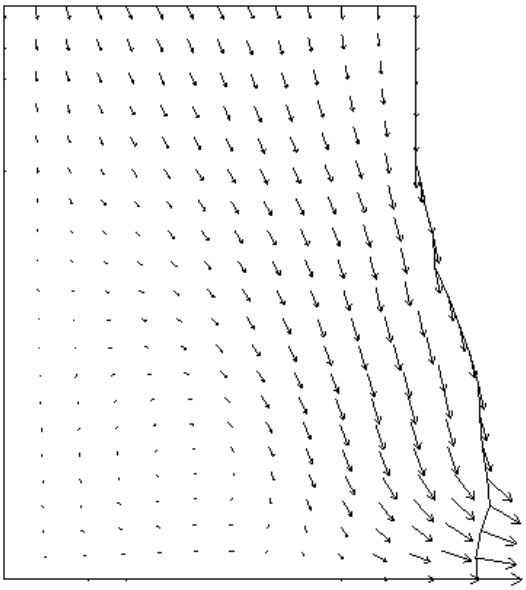

Fig. 4. Nodal velocity field at 10% reduction.

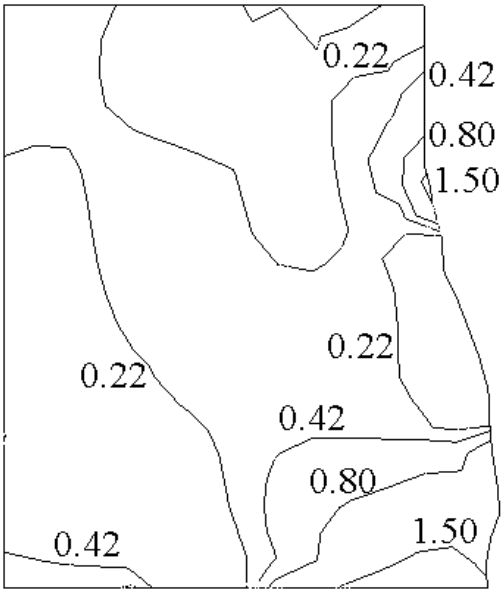

Fig. 6. Equivalent strain rate (1/s) at 10% reduction.

half of the workpiece is calculated owing to symmetry. As seen in these figures, the nodal velocities of the center zone near to the lower die are low, at both the reduction cases.

Figs. 5 and 6 show contours of equivalent strain rate at 6% reduction and 10% reduction, respectively. As seen in these figures, the equivalent strain rates of the zones near to the corners of the upper die and the outer zones near to the lower die are larger, at both the reduction cases.

Figs. 7 and 8 show contours of equivalent strain at 6% reduction and 10% reduction, respectively. As seen in these figures and Figs. 5 and 6, the distributions of the

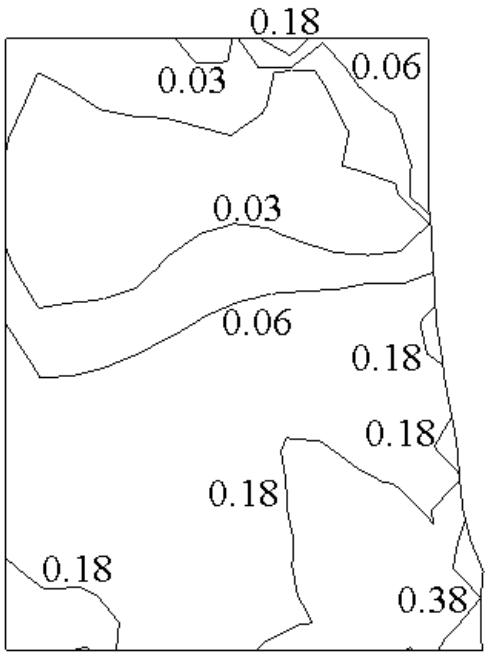

Fig. 7. Equivalent strain at 6% reduction.

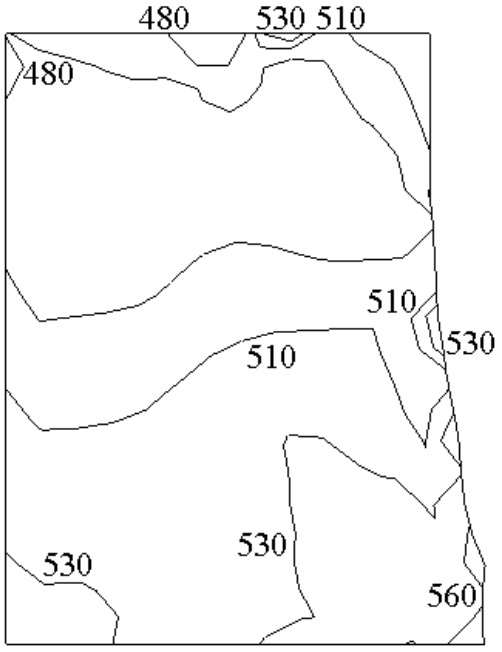

Fig. 9. Equivalent stress (MPa) at 6% reduction.

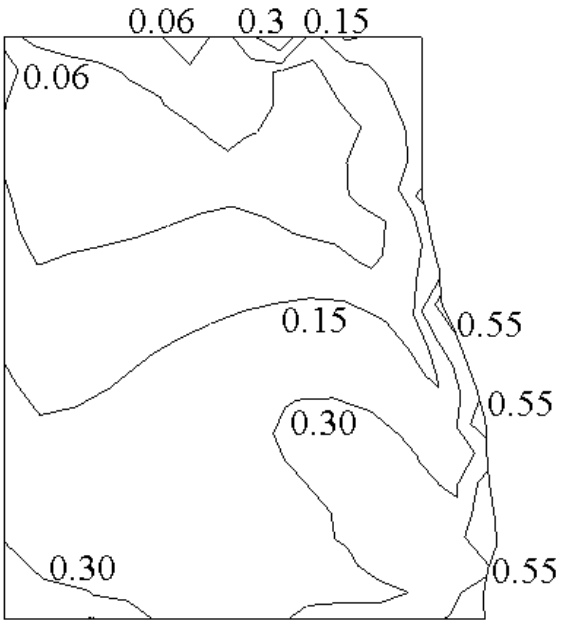

Fig. 8. Equivalent strain at 10% reduction.

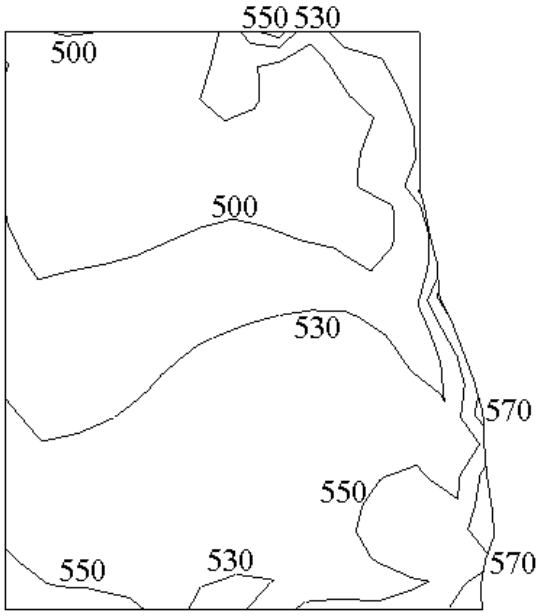

Fig. 10. Equivalent stress (MPa) at 10% reduction.

equivalent strain are similar to those of the equivalent strain rate, the equivalent strain of the outer zones near to the lower die are larger at 6% reduction, and the equivalent strain of the zones near to the corners of the upper die and the outer zones near to the lower die are larger at 10% reduction.

Figs. 9 and 10 show contours of equivalent stress at 6% reduction and 10% reduction, respectively. As seen in these figures and Figs. 7 and 8, the distributions of the equivalent stress are similar to those of the equivalent strain, the equivalent stress of the outer zones near to the

lower die are larger at 6% reduction, and the equivalent stress of the zones near to the corners of the upper die and the outer zones near to the lower die are larger at 10% reduction.

4 Conclusion

The axisymmetric forging problem is analyzed by using the rigid-plastic hybrid PCM/FEM. By introducing a boundary layer of finite element in boundary domain of analyzed body, unsatisfactory issue of the positivity conditions of boundary points in the PCMs can be avoided, and the complicated boundary conditions can be easily imposed with the boundary layer of finite element. By making such an improvement, the hybrid PCM/FEM can be used for analyzing problems of forming effectively.

In addition, the modified MLS approximation is used in this paper; its shape functions have Kronecker-delta property. Then, the unsatisfactory issue of the essential node condition of the classical MLS approximation can be avoided in the modified MLS approximation.

References:

[1] C.H. Lee and S. Kobayashi, New solutions to rigid-plastic deformation problems using a matrix method, *Trans. ASME, J. Engrg. Industry*, Vol.95, 1973, pp.865-873.

[2] B. Nayroles, G. Touzot and P.Villon, Generalizing the FEM: diffuse approximation and diffuse elements, *Computational Mechanics*, Vol.10, 1992, pp.307-318.

[3] T. Belytschko, Y.Y. Lu and L.Gu, Element free Galerkin methods, *Int. J. Numer. Methods Engrg.*, Vol.37, 1994, pp.229-256.

[4] W.K. Liu, S. Jun, S. Li, J. Adee and T. Belytschko, Reproducing kernel particle methods for structural dynamics, *Int. J. Numer. Methods Engrg.*, Vol.38, 1995, pp.1655-1679.

[5] C.A. Duarte and J.T. Oden, An h-p adaptive method using clouds, *Comput. Methods Appl. Mech. Engrg.*, Vol.139, 1996, pp.237-262.

[6] J.M. Melenk and I. Babuska, The partition of unity finite element method: basic theory and applications, *Comput. Methods Appl. Mech. Engrg.*, Vol.139, 1996, pp.289-314.

[7] E. Onate, S. Idelsohn, O.C. Zienkiewicz and R.L. Toylor, A finite point method in computational mechanics. Applications to convective transport and fluid flow, *Int. J. Numer. Methods Engrg.*, Vol.39, 1996, pp.3839-3866.

[8] T. Zhu, J. Zhang and S.N. Atluri, A local boundary integral equation (LBIE) method in computational mechanics and a meshless discretization approach, *Computational Mechanics*, Vol.21, 1998, pp.223-235.

[9] S.N. Atluri and T. Zhu, A new meshless local Petrov-Galerkin (MLPG) approach in computational mechanics, *Computational Mechanics*, Vol.22, 1998, pp.117-127.

[10] E. Onate, S. Idelsohn, O. C. Zienkiewicz, R. L. Toylor and C. Sacco, A stabilized finite point method for analysis of fluid mechanics problems, *Comput. Methods Appl. Mech. Engrg.*, Vol.139, 1996, pp.315-346.

[11] N. R. Aluru, A point collocation method based on reproducing kernel approximations, *Int. J. Numer. Methods Engrg.*, Vol.47, 2000, pp.1083-1121.

[12] X. Jin, G. Li and N.R. Aluru, Positivity conditions in meshless collocation methods, *Comput. Methods Appl. Mech. Engrg.*, Vol.193, 2004, pp.1171-1202.

[13] B. Boroomand, A.A. Tabatabaci and E. Onate, Simple modifications for stabilization of the finite point method, *Int. J. Numer. Methods Engrg.*, Vol.63, 2005, pp.351-379.

[14] M. F. Patricio and P. M. Rosa, Numerical solution of a singularly perturbed two-point boundary-value problem using collocation, *Proc. 8th WSEAS Int. Conf. Applied Mathematics*, 2005, pp.25-30.

[15] S. N. Atluri, H. T. Liu and Z. D. Han, Meshless local Petrov-Galerkin (MPLG) mixed collocation method for elasticity problems, *Computer Modeling Engrg. Sciences*, Vol.14, 2006, pp.141-152.

[16] S. N. Atluri, H. T. Liu and Z. D. Han, Meshless local Petrov-Galerkin (MPLG) mixed finite difference method for solid mechanics, *Computer Modeling Engrg. Sciences*, Vol.15, 2006, pp.1-16.

[17] S. Li and S. N. Atluri, Topology-optimization of structures based on the MPLG mixed collocation method, *Computer Modeling Engrg. Sciences*, Vol.26, 2008, pp.61-74.

[18] S. Chantasiriwan, Performance of multiquadric collocation method in solving lid-driven cavity flow problem with low Reynolds number, *Computer Modeling Engrg. Sciences*, Vol.15, 2006, pp.137-146.

[19] P. H. Wen and Y. C. Hon, Geometrically nonlinear analysis of Reissner-Mindlin Plate by

meshless computation, *Computer Modeling Engrg. Sciences*, Vol.21, 2007, pp.177-191.

[20] I. Caraus and N. E. Mastorakis, Convergence of the collocation methods for singular integro-differential equations in Lebesgue spaces, *WSEAS Trans. Mathematics*, Vol.6, 2007, pp.859-864.

[21] I. Caraus and N. E. Mastorakis, The stability of the collocation methods for approximate solution of singular integro-differential equations, *WSEAS Trans. Mathematics*, Vol.7, 2008, pp.121-129.

[22] G. Kosec and B. Sarler, Local RBF collocation method for Darcy flow, *Computer Modeling Engrg. Sciences*, Vol.25, 2008, pp.197-207.

[23] C.-P. Wu, K.-H. Chiu and Y.-M. Wang, A mesh-free DRK-based collocation method for the coupled analysis of functionally graded magneto-electro-elastic shells and plates, *Computer Modeling Engrg. Sciences*, Vol.35, 2008, pp.181-214.

[24] C. Yang, D. Tang, C. Yuan, W. Kerwin, F. Liu, G. Canton, T. S. Hatsukami and S. N. Atluri, Meshless generalized finite difference method and human carotid atherosclerotic plaque progression simulation using multi-year MRI patient-tracking data, *Computer Modeling Engrg. Sciences*, Vol.28, 2008, pp.95-107.

[25] S. Spanulescu and M. Moldovan, Effects of a supplementary quadrature in the collocation method for solving the Hartree Fock equations in Ab-initio calculations, *WSEAS Trans. Mathematics*, Vol.8, 2009, pp.11-20.

[26] A. J. Khattak, S. I. A. Tirmizi and S.-ul-Islam, Application of meshfree collocation method to a class of nonliear partial differential equations, *Engrg. Analysis Boundary Elements*, Vol.33, 2009, pp.661-667.

[27] Y. C. Hon and Z.-H. Yang, Meshless collocation method by Delta-shaped basis functions for default barrier model, *Engrg. Analysis Boundary Elements*, Vol.33, 2009, pp.951-958.

[28] Z. EI Zahab, E. Divo and A. J. Kassab, A localized collocation meshless method (LCMM) for incompressible flows CFD modeling with applications to transient hemodynamics, *Engrg. Analysis Boundary Elements*, Vol.33, 2009, pp.1045-1061.

[29] Z. Wieckowski, Plenary Lecture 8: The Material Point Method in Large Strain Problems, *Proc. 11th WSEAS Int. Conf. Mathematical Computational Methods Science Engrg.*, 2009, p.21.

[30] S. V. Patanakar, *Numerical Heat Transfer and Fluid Flow*, Hemisphere, 1980.

[31] L. Demkowicz, A. Karafilt and T. Liszka, On some convergence results for FDM with irregular mesh, *Comput. Methods Appl. Mech. Engrg.*, Vol.42, 1984, pp.343-355.